[6]W. R. Smythe, "Charged Right Circular Cylinder," J. Appl. Phys. **33**, 2966–2967 (1962); P. C. Waterman, "Matrix Methods in Potential Theory and Electromagnetic Scattering," J. Appl. Phys. **50**, 4550–4566 (1979); B. D. Popović, M. B. Dragović, and A. R. Djordjević, *Analysis and Synthesis of Wire Antennas* (Research Studies Press, Chichester, 1982); P. K. Wang, "Calculation of Electrostatic Fields Surrounding Finite Circular Cylindrical Conductors," IEEE Trans. Antennas Propag. **32**, 956–962 (1984); A. R. Djordjević, "Comments on 'Calculation of Electrostatic Fields Surrounding Finite Circular Cylindrical Conductors,' " IEEE Trans. Antennas Propag. **33**, 683–684 (1985); P. K. Wang, C. H. Chuang, and N. L. Miller, "Electrostatic, Thermal and Vapor Density Fields Surrounding Stationary Columnar Ice Crystals," J. Atmos. Sci. **42**, 2371–2379 (1985).

[7]W. R. Smythe, Ref. 2, p. 209.

[8]A. R. Djordjević, personal communication.

[9]Material in this section is based on Ye Li's unpublished Reed College senior thesis (1994).

[10]The electrical force on the *outermost* charges (at $\pm a$) is *not* zero, of course, because they are subject to the extra constraining force holding the charges on the wire. By the way, one can (equivalently) calculate the total *potential energy* of the configuration, and minimize it to determine the positions of the charges.

[11]J. B. Ross, "Plotting the charge distribution of a closed-loop conducting wire using a microcomputer," Am. J. Phys. **55**, 948–950 (1987). Ross used the potential *at* each charge (due to all the others), but for open segments it is better to use the midpoints, since the end charges are subject to nonelectrostatic forces.

[12]Smythe, Ref. 2, Sec. 4.22.

[13]This result can also be obtained by treating the ribbon as the limiting case of an elongated ellipsoid. With $\Lambda \equiv Q/2c$ and $c \to \infty$, Eqs. (2.1) and (2.2) yield

$$\sigma(x) = \frac{\Lambda}{\pi}\left[a^2 - x^2 + \left(\frac{bx}{a}\right)^2\right]^{-1/2}.$$

This is the net surface charge density (both sides) for an infinite cylinder of elliptical cross section. In the limit $b \to 0$ it reduces to a ribbon, and we recover Eq. (4.6). [In the case $c = \infty$, the analog to the theorem in Sec. II A states that the charge per unit length (in the z direction) on a strip of width dx is $\Lambda dx/(\pi\sqrt{a^2 - x^2})$ for all b—but (unlike the *finite* ellipsoid) it is *not* independent of x.]

[14]It is easy to check that the total linear charge density $[\int \sigma(x)dx]$ is Λ.

[15]We have pushed the fixed-position bead model up to $n = 300$ with barely detectable changes in the curve; the best fit of the form (3.7) occurs for $A = 0.384049$, $B = 0.088295$.

[16]This method cannot be applied to the Coulomb problem, of course, because of the nasty singularity in the integrand.

Electric field line diagrams don't work

Alan Wolf[a)]
Department of Physics, The Cooper Union, New York, New York 10003

Stephen J. Van Hook,[b)] Eric R. Weeks[c)]
Center for Nonlinear Dynamics, Department of Physics, The University of Texas, Austin, Texas 78712

(Received 27 July 1995; accepted 10 December 1995)

Electric fields produced by coplanar point charges have often been represented by field line diagrams that depict two-dimensional slices of the three-dimensional field. Serious problems with these "conventional" field line diagrams (CFLDs) have been overlooked. Two of these problems, "equatorial clumping" and "false monopole moment," occur because a two-dimensional slice lacks information vital to the accurate representation of an inherently three-dimensional field. Equatorial clumping causes most CFLDs to exhibit unphysical behavior such as irregular spacing between field lines terminating on negative charges. CFLDs can also mistakenly indicate that a neutral charge distribution has a significant monopole moment. Such phenomena make the visual estimation of local field strengths impossible and render CFLDs of little utility for representing three-dimensional fields. While these "projection" problems can be avoided by using two-dimensional field line diagrams to represent two-dimensional ($1/r$) electric fields, or by using three-dimensional field line diagrams to represent three-dimensional fields, other forms of distortion generally remain.

I. INTRODUCTION

Elementary physics textbooks generally attempt some form of two-dimensional graphical representation of the three-dimensional electric field produced by coplanar point charges. The most common approach, the conventional field line diagram (CFLD), employs continuous electric field lines, or "lines of force," which are everywhere tangent to the electric field. Each field line is traced from a positive charge until it terminates on a negative charge or at infinity (i.e., "far" from all charges). An individual field line conveys information about the local direction of the electric field, but not about the field's magnitude. The latter property requires consideration of the local density of field lines. Figure 1(a), for example, illustrates the CFLD for a simple dipole. Field lines near the dipole are generally spaced close together, which is thought to indicate a high field strength, while more distant lines are spaced farther apart. The tendency of the field line density to decrease with distance from the dipole is apparently consistent with the asymptotic $1/r^3$ decay of the field strength. Field lines are, of course, creatures of fiction.[1] However CFLDs such as Fig. 1(a) are gen-

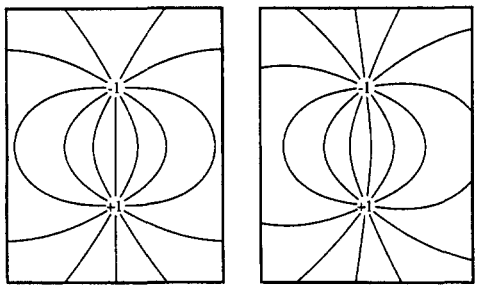

(a) (b)

Fig. 1. Conventional field line diagram (CFLD) for a dipole. (The sign and magnitude of each charge appear in the circular region surrounding the charge. Field lines are initiated much closer to positive charges than the size of the circular regions appears to suggest.) (a) The symmetry of the field is made apparent by setting the starting angle for field line emission, θ_0, equal to 0. (b) The symmetry is hidden by choosing an arbitrary value for θ_0.

erally thought to be useful, since it is believed that they allow, by direct inspection, estimation of the electric field's local direction and local magnitude.

Textbooks sometimes note that field line density is proportional to field strength in three dimensions, but rarely address the relationship between these quantities in the two-dimensional diagrams actually used for field visualization. The reader is left to infer that a similar, if not identical, relationship holds in two dimensions.[2] In fact, in almost every CFLD, *field strength has no consistent relationship to the observed field line density*. While several phenomena contribute to this result, we focus here on a particular type of distortion which we call "equatorial clumping." It is well known that field line diagrams imperfectly represent electric fields in relatively minor ways,[3] but the more disturbing effect of equatorial clumping has not been reported in the electromagnetism literature. While field line density and field strength are not related in any simple fashion in a CFLD, individual field lines are, by definition, tangent to the local electric field. Therefore, CFLDs, while failing to accurately reflect a field's local magnitude, do correctly report its local direction.

Section II examines the theoretical relationship between field line density and field strength. Our computational scheme for producing CFLDs is outlined in Sec. III. Equatorial clumping is discussed in Sec. IV. Equatorial clumping is infrequently seen in textbook figures, for the simple reason that textbooks generally illustrate only monopole and dipole fields, which do not exhibit the effect. Since most point charge distributions (including the simple quadrupole) do manifest equatorial clumping, the absence of this effect in more ambitious textbook figures suggests that these CFLDs are artist's renderings, not the result of an analytical calculation[4] or a numerical computation such as the one outlined in Sec. III. Equatorial clumping is also observed in the CFLDs produced by some educational software.[5]

Equatorial clumping derives from the fact that a two-dimensional slice of a three-dimensional vector field lacks information vital to an accurate representation of the field. For ease of reference we refer to this loss of information as a "projection" effect, although, strictly speaking, a slice is not equivalent to a projection. Section V looks at another projection effect, the appearance of spurious monopole moments in CFLDs. Section VI considers two methods for avoiding projection effects by avoiding the use of a slice. Unfortunately,

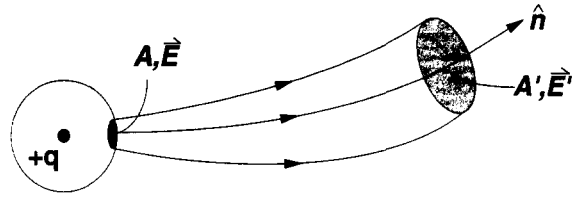

Fig. 2. Gaussian tube encircles some of the field lines emitted by a positive charge. Gauss' law relates the field strength, E, the area A, and the three-dimensional field line density, ρ.

even if one of these methods can be employed, another significant form of graphical distortion, which we call "boundary clumping," will often remain. This effect, which also thwarts attempts to visually estimate local field strength, is discussed in Sec. VII. Section VIII considers the problems associated with the use of three-dimensional rather than two-dimensional field line diagrams. The authors conclude that electric fields are not well represented by graphical techniques that employ continuous lines of force.

II. RELATING FIELD LINE DENSITY TO FIELD STRENGTH

The relationship between field line density and field strength is determined by Gauss' law:

$$\oint (\mathbf{E}\cdot\hat{n}\, dA) = 4\pi q_{\text{enclosed}}, \tag{1}$$

where the integral is taken over a closed Gaussian surface enclosing net charge q_{enclosed}, $\hat{n}$ is an outward-drawn unit normal to the surface, and CGS units are used. To relate field line density to field strength we select as our Gaussian surface the narrow closed tube shown in Fig. 2. To prevent field lines from leaving the tube along its length, the "sides" of the tube are chosen to be everywhere tangent to the electric field. The ends of the tube are oriented perpendicular to the field. The tube encircles a large but finite number of field lines, each of which begins on the positive point charge of magnitude q, and terminates at infinity or on a negative charge.

As the field is uniform over each end of the tube (A and A' are assumed small), and no charge is enclosed,

$$\oint (\mathbf{E}\cdot\hat{n}\, dA) = -EA + E'A' = 4\pi q_{\text{enclosed}} = 0, \tag{2}$$

so that

$$EA = E'A'. \tag{3}$$

To represent the electric field by a three-dimensional field line diagram, we first select a value for N, the number of field lines emitted by a positive charge of unity magnitude. We then uniformly distribute qN field lines over the surface of an infinitesimal sphere surrounding the point charge (the question of when uniformity can be achieved is deferred until Sec. VIII). The number of field lines entering the tube is given by ρA, where ρ, the field line density, is defined as the number of field lines per unit area. Since no field lines escape through the walls of the tube,

$$\rho A = \rho' A'. \tag{4}$$

Combining Eqs. (3) and (4), we obtain

$$E' = \rho'(E/\rho) \propto \rho'. \tag{5}$$

Thus, the density of field lines penetrating a surface with normal $\hat{n}$ is proportional to the strength of the field in the $\hat{n}$ direction, or

$$\mathbf{E}(\mathbf{x}) \cdot \hat{n} \propto \rho(\mathbf{x}, \hat{n}). \tag{6}$$

Since Gauss' law gives rise to Eq. (6), the proportionality between field line density and field strength is an inherently three-dimensional result. In principle, Eq. (6) permits the visual estimation of local field strength in a three-dimensional field line diagram. Three-dimensional field line diagrams are rarely used, however, since two-dimensional renderings of such diagrams are difficult or impossible to interpret.

One might assume that the field line density in a CFLD, a two-dimensional slice of three-space, would proportionally reflect the density of field lines in three-space. If this were true, Eq. (6) would indirectly permit the visual estimation of field strength in a CFLD. The assumption may seem plausible because the CFLD, drawn in the plane that contains the charge distribution, possesses the unique property that field lines starting in the plane remain within it and no other field lines enter the plane. This property may suggest that local field line densities in the CFLD reflect (i.e., are proportional to) the three-dimensional field line density appearing in Eq. (6). Unfortunately, however plausible this assumption may seem, it is incorrect.

While Eq. (6) defines a global linear relationship between field strength and three-dimensional field line density, there is no consistent relationship between field strength and field line density in a CFLD. This is explained in part by phenomena such as equatorial clumping, which misrepresent local field strength to varying degrees in different regions of a CFLD. It is easily demonstrated, however, that even if local distortions were absent, no global relationship is possible. Consider the CFLD associated with an isolated positive charge. The charge, by virtue of emitting qN field lines, will produce a certain field line density at a distance d. If q is doubled, the charge emits twice as many field lines,[6] doubling the density. Since the strength of the field is proportional to the magnitude of the charge, it appears that field strength and two-dimensional field line density are linearly related. Suppose, however, that d, rather than q, is doubled. The field strength, which decays as $1/r^2$, decreases by a factor of 4. The field lines, linearly diverging within the plane of the CFLD, double their separation in traveling the additional distance, decreasing the density by a factor of 2. The latter experiment suggests that field strength and two-dimensional field line density are quadratically related. Since the linear and the quadratic relationship cannot both be satisfied, the two quantities cannot share *any* consistent relationship.

Even if one has not been taught that high field line densities in a CFLD reflect high local field strengths, there is a natural tendency to make such an association. Unfortunately, since Eq. (6) does not apply to CFLDs, these visual estimates may be highly inaccurate, even in the case of a simple quadrupole.

III. PRODUCING TWO-DIMENSIONAL FIELD LINE DIAGRAMS

The following computational scheme is used to create CFLDs:

(1) Specify the two-dimensional distribution of point charges.
(2) Specify the number of field lines, N, that represent a charge of unit magnitude. (For example, if $N=12$, a $+2$ charge "emits" 24 field lines, while a -3 charge should "absorb" 36 field lines.)
(3) Initiate field lines very close to each positive charge at uniform angular intervals consistent with the choice of N. (For example, if $N=12$, a $+2$ charge emits one field line every $2\pi/24$ radians.) The use of equal intervals *assumes* uniformity of the field at the starting location; for uniformity to actually be present, the starting location must be close enough to the originating charge that its uniform field dominates the total electric field.
(4) Follow each field line from its starting point until it closely approaches a negative charge or appears to be diverging to infinity. To determine the path of a field line, first compute the x and y components of the total field at the current location from the point charge contributions, $q_i \hat{r}_i / r_i^2$. Then incrementally advance the field line, parametrized by arclength s, by solving the differential equations: $dx/ds = E_x/|E|$, $dy/ds = E_y/|E|$ (E_z is zero in the plane of the diagram and can be ignored.) Dynamic adjustment of the integration stepsize will allow relatively sharp turns in field lines, such as occur at "saddle points" where $E=0$, to be accurately followed.

While the choice of N determines the angular spacing between field lines, the overall angular orientation of the emission pattern of field lines is determined by the starting angle, θ_0,[7] selected for each positive charge. While the θ_0's are computationally arbitrary, some choices may be better than others. For example, in the dipole field illustrated in Fig. 1(a), the choice $\theta_0=0$ (which places the first outgoing field line at the 12 o'clock position) results in field lines symmetric about the y axis, consistent with the azimuthal symmetry actually present in the three-dimension field. In Fig. 1(b) the symmetry of the field has been hidden by slightly decreasing θ_0. For an arbitrary, asymmetric charge distribution, the phenomenon of "hidden field symmetries" cannot occur. However charge distributions of pedagogical interest, i.e., a multipole or parallel lines of point charges, often possess some type of symmetry. In such cases poor choices for each θ_0 will result in CFLDs that do not reflect that symmetry.

An apparent problem with our computational scheme is that it omits all of the field lines that begin at infinity. In a charge distribution containing solely negative charges, for example, this scheme produces no field lines at all. The problem of missing field lines is easily remedied by reversing the sign of each charge in the distribution, so the number of field lines emitted in the CFLD is no smaller than the number of lines absorbed. This modification of the charge distribution should not change any field properties that are correctly reflected in the field line diagram, since charge reversal only brings about a global reversal in the direction of the electric field.

IV. EQUATORIAL CLUMPING

Figure 3 illustrates the phenomenon of "equatorial clumping" for a simple point charge distribution. Field lines emitted uniformly from the $+1$ and $+3$ charges terminate nonuniformly on the -4 charge. The nonuniformity is more apparent in Fig. 4, a 32-fold magnification of the region near the negative charge. If Eq. (6) were thought to apply to Fig.

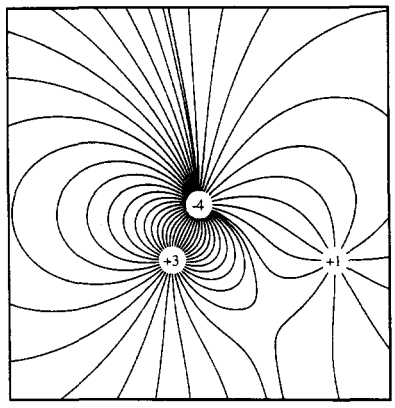

Fig. 3. CFLD for a coplanar point charge distribution demonstrating "equatorial clumping," the nonuniform spacing of field lines that should terminate uniformly on the negative charge.

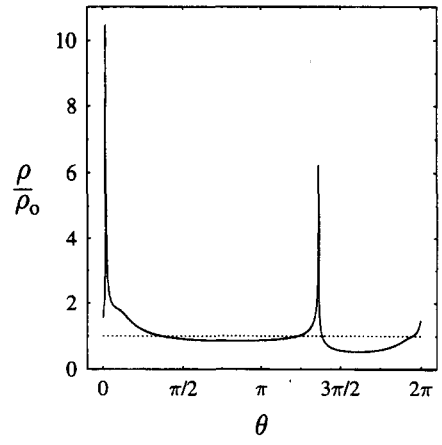

Fig. 5. The angular density of 40 000 field lines terminating on the negative charge of Fig. 4. The angular range begins at the 12 o'clock position, and proceeds counterclockwise around the charge. The density has been scaled by the uniform density (indicated by a dashed line) that would be observed if there were no equatorial clumping.

4, one would mistakenly conclude that the electric field very close to the negative charge was weaker in the "12 to 4 o'clock" range than elsewhere. Figure 5, a plot of the angular density of terminating field lines, provides a more quantitative illustration of the effect. The equatorial clumping evident in Fig. 4 appears in Fig. 5 in the lower angular density in the 12 to 4 o'clock range (approximately $3\pi/2$ to 2π in Fig. 5) than elsewhere. Figure 5 also contains two large spikes, indicating very high field line densities, which are not seen in Fig. 4. The spikes, which span a narrow range in θ, are overlooked by the 48 terminating field lines of Fig. 4, but are picked up by the 40 000 field lines of Fig. 5. This demonstrates that the extent of equatorial clumping actually observed in a CFLD depends on the choice of N, which proportionally alters the local field line density, ρ.

Equation (6), if used to interpret Figs. 3–5, would provide misleading information about the magnitude of the field in the vicinity of the -4 charge. Sufficiently close to that charge, its nearly infinite, perfectly uniform field must dominate the total field, but uniformity is not seen in the figure. One might have expected that the computational scheme of Sec. III would automatically result in uniformity for the field lines terminating on negative charges, since uniformity was imposed on the field lines emitted by the positive charges.

Equatorial clumping may also provide false information about charge magnitude, which is reflected in a CFLD by the number of field lines attached to each charge. Figure 6 illustrates the field of a linear quadrupole, with charges $+2$, -4, and $+2$, for $N=9$. While equatorial clumping, i.e., an increase in field line density, is apparent near the "equator" of the -4 charge, the expected number of field lines are attached to each charge—18 lines begin on each positive charge and 36 lines terminate on the negative charge. In Fig. 7, the -4 charge is replaced by a small cluster of -1 charges, two on the x axis ("equatorial charges"), and two on the y axis ("polar charges"). While each -1 charge should absorb nine field lines, the incoming field lines continue to express their preference for landing in the equatorial region of the "-4" charge. Each equatorial charge absorbs 11 field lines and each polar charge absorbs seven field lines. Inspecting the field line diagram, one would incorrectly conclude that the magnitude of the equatorial charges exceeds that of the polar charges by the ratio 11:7.[8]

The calculational degrees of freedom in our CFLD algorithm are easily ruled out as the source of equatorial clumping. As Fig. 5 demonstrates, increasing the field line density to better represent the continuous nature of the vector field only makes equatorial clumping more apparent. Varying the starting angles similarly has no effect on density plots such

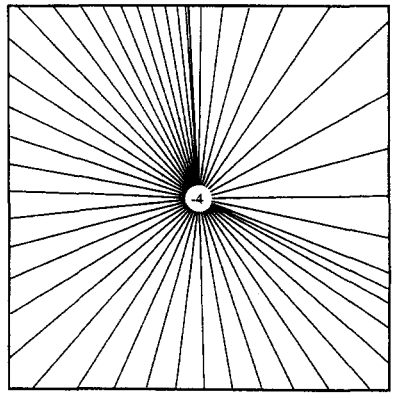

Fig. 4. Thirty-two-fold magnification of the negative charge in Fig. 3 emphasizing the nonuniform termination of field lines.

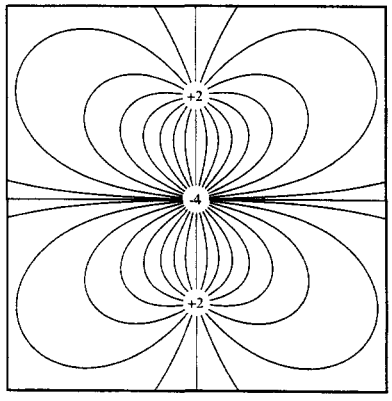

Fig. 6. CFLD for a linear quadrupole, with equatorial clumping evident near the equator of the negative charge.

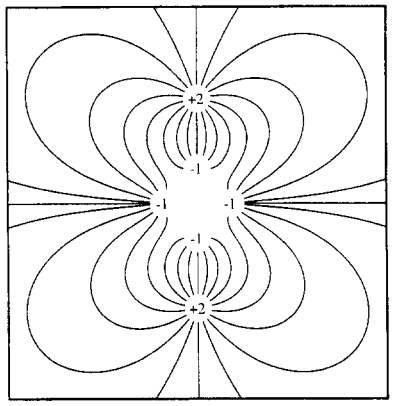

Fig. 7. CFLD for a charge distribution similar to the linear quadrupole of Fig. 6. Equatorial clumping causes the wrong number of field lines to terminate on the negative charges. Each +2 charge emits 18 field lines; the polar and equatorial −1 charges absorb, respectively, 7 and 11 field lines.

as Fig. 5. (Section VII considers a different type of CFLD distortion which is affected by the choice of starting angles.) Finally, equatorial clumping is not affected by the choice of starting distances for field lines, so long as this distance is sufficiently small.

Numerical errors are also easily ruled out as the source of equatorial clumping. No change in clumping is observed when the integration stepsize is reduced or when the Eulerian integration scheme is replaced by a fourth-order (Runge–Kutta) method. Furthermore, each terminating field line returns to its point of origin to very high accuracy when integrated backward.

Equatorial clumping results, instead, from a projection effect; CFLDs, which are two-dimensional, cannot accurately represent inherently three-dimensional electric fields. This explanation is easily confirmed by producing a three-dimensional field line diagram for the linear quadrupole, by extension of the scheme outlined in Sec. III. No equatorial clumping is observed in three dimensions—field lines uniformly emitted from positive charges are uniformly absorbed on negative charges. Since three-dimensional field line diagrams are not easy to interpret visually, the absence of equatorial clumping is best verified numerically. When dense groups of field lines are initiated from regions of small but equal solid angle, $d\Omega_+ = d(\cos\theta)d\phi$, on a spherical surface surrounding a positive point charge, they land in regions of equal solid angle, $d\Omega_- = d\Omega_+ |q_+/q_-|$, on a spherical surface surrounding a negative charge.

The behavior of such field line groups describes a mapping of regions of solid angle from positive to negative charges. This mapping, while area-preserving (up to the factor $|q_+/q_-|$), is not shape preserving. In particular, when terminating field lines are compressed in the θ direction in the equatorial region, they stretch in the ϕ direction. Since θ lies within the plane of the diagram, but ϕ is perpendicular to this plane, the compression, or "clumping" of field lines is retained in the two-dimensional slice, but the compensatory stretching is discarded.

This projection effect is easily quantified for the linear quadrupole. A portion of the quadrupole CFLD is shown in Fig. 8(a); the behavior of the corresponding field lines in three dimensions is illustrated schematically in Fig. 8(b). Consider the field lines emanating from infinitesimal circular endcaps of equal solid angle, Ω, near the north and south

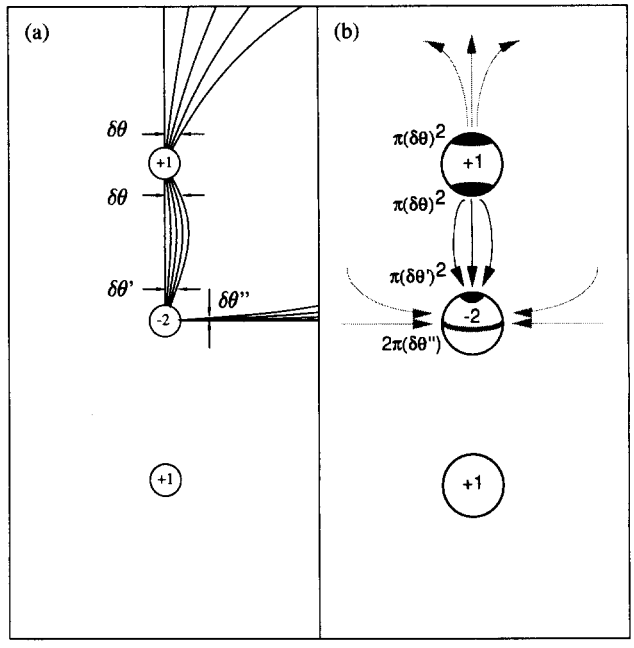

Fig. 8. Field lines initiated on the south and north poles of a positive charge in a linear quadrupole terminate, respectively, on the north pole and an equatorial ring of the negative charge. (a) In a two-dimensional slice of the field the field lines are emitted in an angular range $\delta\theta$ and terminate in angular ranges $\delta\theta'$ and $\delta\theta''$. (b) In three dimensions the field lines are emitted from infinitesimal circular endcaps of solid angle $\pi(\delta\theta)^2$ and terminate in regions of solid angle $\pi(\delta\theta')^2$ and $2\pi(\delta\theta'')$.

poles of the upper +1 charge. From the symmetry of the charge distribution, field lines leaving the south pole must terminate within a north polar endcap on the negative charge. Similarly, field lines leaving the north pole must terminate within a small ring just above the equator of the −2 charge. Since, on the surface of their respective spheres, the field strength produced by the −2 charge is twice that of the +1 charge, Gauss' law requires that the terminating circular endcap and the terminating ring each occupy the solid angle $\Omega/2$. The solid angles of each element are

$$\text{outgoing endcaps:} \quad \pi(\delta\theta)^2 = \Omega, \tag{7}$$

$$\text{terminating endcap:} \quad \pi(\delta\theta')^2 = \Omega/2, \tag{8}$$

$$\text{terminating ring:} \quad 2\pi(\delta\theta'') = \Omega/2, \tag{9}$$

where all angles are expressed in radians. Solving these equations, we find:

$$\frac{\delta\theta''}{\delta\theta'} = \frac{\delta\theta}{2^{3/2}} \ll 1. \tag{10}$$

In three dimensions, therefore, the angular width of the equatorial ring may be much narrower than that of the endcap. The large (azimuthal) girth of the ring compensates for this, ensuring that the terminating solid angles are identical. Gauss' law therefore ensures uniformity in three dimensions. In the two-dimensional projection of Fig. 8(a), however, the broad girth of the negative charge is invisible. Field lines originate in the plane within an angular range $\delta\theta$, and terminate in the plane, in angular ranges $\delta\theta'$ and $\delta\theta''$. In two dimensions Eq. (10) shows that field lines landing near the equatorial region arrive in a far narrower angular range than the identical number of field lines landing near a pole. An arbitrarily large amount of equatorial field line compression

is theoretically possible for sufficiently small $\delta\theta$; however in practice, as Figs. 4 and 5 demonstrate, a limited amount of equatorial clumping will be observed, the precise amount being determined by N (which fixes $\delta\theta$) and θ_0.

In sum, equatorial clumping results from the inability of a two-dimensional field line diagram to properly represent the manner in which regions of solid angle are mapped from positive to negative charges. While this mapping preserves solid angles, it does not always preserve their shapes. Shape variations are obscured in two-dimensional projection, resulting in the field line nonuniformity that we call equatorial clumping.

Equatorial clumping will be present in most field line diagrams, although it is sometimes a subtle effect that is only made apparent by an angular density plot such as Fig. 5. A handful of charge distributions, such as the ordinary dipole, show no equatorial clumping due to their special symmetries. In the dipole, the electric field is unchanged under the combined operations of charge reversal and reflection across a symmetry line (the perpendicular bisector of the line connecting the charges). This symmetry forces any field line reaching the symmetry line from a positive charge to complete its trip to the negative charge in mirror image fashion. Since the emission pattern from the positive charge is perfectly uniform, the mirror image pattern of terminating field lines on the negative charge will be equally uniform. This argument fails for the linear quadrupole, even though it has the identical symmetry under charge reversal and reflection, since field lines do not cross the symmetry line in completing their trip from a positive charge to a negative one. Rather than mirroring the uniform emission pattern, the terminating field lines below the symmetry line mirror the nonuniform termination pattern above the symmetry line. Another charge distribution with sufficient symmetry under the operations of spatial reflection and charge reversal to avoid equatorial clumping consists of the charges $+1$, -1, $+1$, and -1 placed on the consecutive corners of a square.[9] Arbitrary charge distributions will generally lack the high degree of symmetry necessary to eliminate equatorial clumping. The reader is reminded that, even if equatorial clumping is absent, no consistent relationship exists between field strength and field line density in a CFLD.

For collinear charge distributions such as the quadrupole, equatorial clumping will occur when solid angle is mapped between regions of dissimilar girth. In the dipole, polar regions map to polar regions, and equatorial regions map to equatorial ones. In the quadrupole, by contrast, polar regions are mapped to both polar and equatorial regions. Even if a mapping does occur between regions of equal girth, however, equatorial clumping may still be present, though manifested in a different form. This is demonstrated in Fig. 9, a linear quadrupole in which the -2 charge has been synthesized from two -1 charges. While the field lines terminate uniformly on each of the -1 charges, equatorial clumping is still apparent in the nonuniform spacing of field lines in the region between the negative charges. Since equatorial clumping is not limited to terminating field lines, but can occur in charge-free regions of space, the effect may even be present in field line diagrams containing only positive charges. In an arbitrary charge distribution, the mapping analysis is more complex, and equatorial clumping is perhaps a misnomer, since there is no meaningful identification of polar and equatorial directions. We nevertheless retain this terminology, as it conveys the essential point of a mapping that is area-preserving, but not shape-preserving.

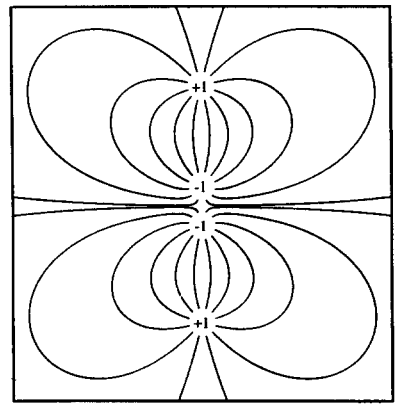

Fig. 9. CFLD for a charge distribution in which equatorial clumping is manifested by the nonuniform spacing of field lines in a charge-free region of space (between the two -1 charges), rather than at field line terminations.

V. FALSE MONOPOLE MOMENT

Figure 10 illustrates an additional distortion that arises from the representation of a three-dimensional field by a two-dimensional slice. Although the charge distribution has no net charge, 25% of the field lines diverge to infinity, incorrectly suggesting that the distribution possesses a net monopole moment.[10]

To understand the appearance of a "false monopole moment" recall that the charge distribution lies within the plane of the CFLD, making the plane a reflection symmetry plane for the three-dimensional field line diagram. Because of this symmetry, field lines that start within the plane can never leave it. No such constraint is present on field lines initiated outside the plane, which may freely travel through three space. Where there is no net charge, as in Fig. 10, each field line should terminate on a negative charge, rather than at infinity. However some field lines initiated on the "far" side of each $+1$ charge cannot detour around the $+1$ charge horizontally (within the plane) in order to reach the -4 charge, but must go above or below the $+1$ charge. Field lines ini-

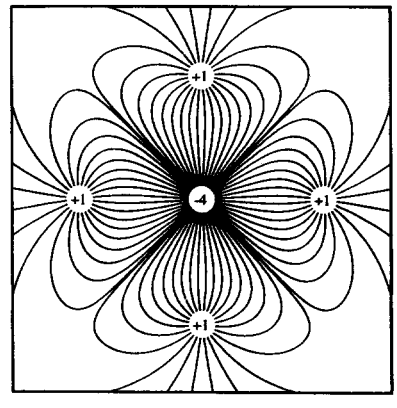

Fig. 10. CFLD for a charge distribution with no net charge. While each field line should terminate on a negative charge within the distribution, 25% of the field lines diverge to infinity, incorrectly suggesting that the distribution possesses a net charge of $+1$.

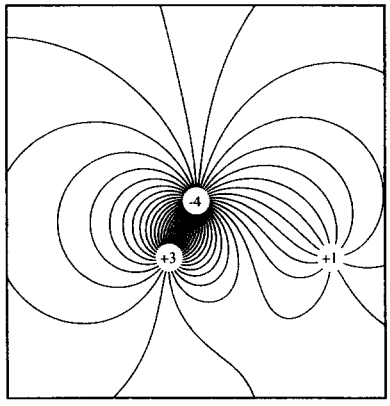

Fig. 11. Field line diagram for the charge distribution of Fig. 3, employing a two-dimensional ($1/r$) electric field to prevent equatorial clumping.

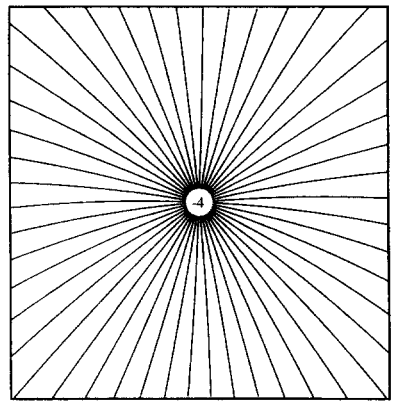

Fig. 12. Thirty-two-fold magnification of the negative charge in Fig. 11 emphasizing the uniform termination of field lines. Compare Fig. 4.

tiated within the symmetry plane cannot take such a three-dimensional detour and have no choice but to go to infinity.

Such diverging field lines are not created by the use of a slice; the identical behavior can be seen in a three-dimensional field line diagram if field lines are initiated within the reflection symmetry plane. In three dimensions, however, the probability of starting a field line precisely within this plane is zero. On the one hand, the reflection symmetry plane is the only plane appropriate for a CFLD, because it is the only plane containing complete (i.e., planar) field lines. On the other hand, the reflection symmetry plane is a poor choice, because planar field lines exhibit atypical field line behavior. It is this atypical behavior, the failure to reach a terminating negative charge, that misinforms as to the net charge present within a distribution.

VI. AVOIDING PROJECTION EFFECTS

Since equatorial clumping and false monopole moments result from taking a two-dimensional slice of a three-dimensional vector field, both effects can be eliminated if the use of a slice can somehow be avoided. One way to accomplish this, through the use of fully three-dimensional field line diagrams, is discussed in Sec. VIII. A different approach involves the use of a two-dimensional, rather than a three-dimensional, electric field. Clearly no information is lost by "projection" if a two-dimensional field line diagram is used to visualize two-dimensional physics.

In two dimensions Gauss' law takes the form:

$$\oint (\mathbf{E}\cdot\hat{n}\, dl) = 2\pi q_{\text{enclosed}}. \tag{11}$$

Here $\hat{n}$ is the local normal to a closed curve, which is the two-dimensional analog to a Gaussian surface. In Sec. IV it was shown that the three-dimensional form of Gauss' law, as expressed in Eqs. (7)–(9), prevented equatorial clumping in three dimensions. In the identical derivation employing two-dimensional physics, which would look to the mapping of field lines between angular regions within the plane, rather than regions of solid angle, Eq. (11) similarly prevents equatorial clumping in two dimensions.

Figures 11 and 12 illustrate the two-dimensional electric field associated with the charge distribution used in Figs. 3 and 4. Equatorial clumping has been eliminated. Unfortunately, the two-dimensional electric field associated with a specified charge distribution differs substantially from the three-dimensional field associated with the same distribution since the field strength varies as $1/r$, instead of $1/r^2$. The use of a two-dimensional field eliminates equatorial clumping, but it does not solve the problem originally posed.

Two-dimensional fields do, however, have at least two potential applications. First, one may take the view that electric field line diagrams are being produced for point charges that exist in a Flatland-like universe with only two spatial dimensions.[11] The pedagogic appeal of this view is that the entirety of the field lies within the plane of the diagram, so that no three-dimensional visualization, calculation, or vector calculus is required. For example, Gauss' law, in its two-dimensional form, is easily applied to relatively complex charge distributions. One disadvantage of two-dimensional electrostatics is that electric potential has a logarithmic spatial dependence, which makes it more difficult to interpret and to represent graphically.

Alternatively, one can view the field as being generated by infinite lines of charge perpendicular to the plane. The symmetry of such a distribution ensures that all field lines are confined to planes perpendicular to the lines of charge, with each plane exhibiting identical field behavior. Furthermore, the field produced by an infinite line of charge varies inversely with the distance from the charge. A slice taken through the three-dimensional electric field therefore reveals purely two-dimensional field behavior, with no information lost by projection. Figure 11 may therefore be interpreted as the field line diagram produced by three point charges residing in two-space, or by three infinite lines of charge perpendicular to the plane of the diagram.

The use of two-dimensional electric fields also avoids the projection effect of false monopole moments. This is illustrated in Fig. 13, the two-dimensional counterpart to Fig. 10.

VII. BOUNDARY CLUMPING

Even if projection effects can be avoided, an entirely unrelated form of distortion may be present in a field line diagram that makes it difficult to correctly extract local field properties. To prevent projection effects from masking this new form of distortion we use two-dimensional electric fields in the figures for this section.

Figure 14 shows the field line diagram associated with a simple collection of point charges. At the 10 o'clock and the 2 o'clock positions on the -3 charge a pair of terminating field lines have an atypically large angular separation, imply-

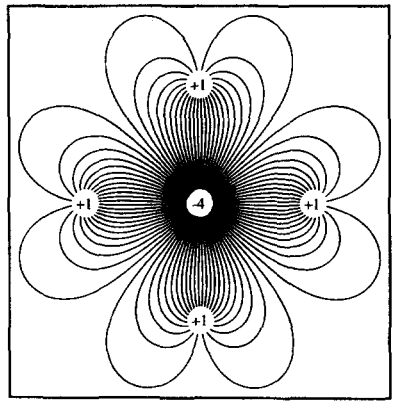

Fig. 13. Field line diagram for the charge distribution of Fig. 10, employing a $1/r$ electric field to prevent the appearance of a false monopole moment.

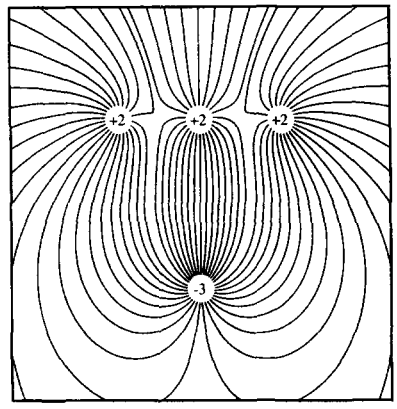

Fig. 14. Field line diagram with $1/r$ field, illustrating "boundary clumping," the nonuniform spacing of isolated pairs of field lines that originate on different positive charges.

ing a reduced local field strength. Some form of distortion must be present here, since the field close to any charge is perfectly uniform. We refer to this distortion as "boundary clumping" because, as Fig. 14 illustrates, irregular spacing appears at the boundaries between terminating field lines that originate on different positive charges.

In Fig. 15, boundary clumping has been eliminated by altering the value of θ_0 in a symmetric fashion on the two outermost positive charges. Since the θ_0's are free parameters in our calculation, it is apparent that boundary clumping does not reflect any real property of the electric field. Furthermore, while boundary clumping is affected by the choice of each θ_0, the effect is otherwise unrelated to hidden field symmetries. This is demonstrated by Fig. 14, which exhibits boundary clumping even though its field lines correctly reflect the symmetry of the charge distribution about the line joining the -3 charge and the central $+2$ charge.

Boundary clumping is not limited to pairs of field lines that terminate on negative charges. In Fig. 14 we also see atypical spacing between two pairs of field lines at the top of the diagram, field lines that originate on different positive charges, and are in the process of diverging to infinity. As Fig. 15 illustrates, when the starting angles are altered to eliminate boundary clumping for field lines terminating on the negative charge, the nonuniformity also disappears for the field lines that diverge.

As with equatorial clumping, boundary clumping may mislead not only as to local field strength, but as to charge magnitude. This phenomenon is illustrated in Fig. 16, in which two -1 charges absorb different numbers of field lines (11 on the upper -1 charge, 13 on the lower) from the two $+1$ charges that emit them. To understand this problem, we observe that it will be difficult for the *finite* number of field lines connecting a positive charge to a negative one to properly reflect the angular range that should be mapped between the two charges, since the range can assume any value from 0 to 2π. In Fig. 16, for example, by choosing $N=12$, the only mappings that can be correctly described are those involving angular ranges that are multiples of $2\pi/12$. Mapped regions will not generally have sizes that are integer multiples of $2\pi/12$; in this circumstance, boundary clumping can cause the wrong number of field lines to land on negative charges. For example, if the size of the angular region that maps from a $+1$ charge to a -1 charge were equal to $8.5\cdot 2\pi/12$, then depending on θ_0 for the $+1$ charge, either 8 or 9 field lines could map from the positive to the negative charge. If another $+1$ charge contributes the remaining angular range of $3.5\cdot 2\pi/12$, then depending on θ_0 for that charge, either 3 or 4 field lines could map to the negative charge. Since the starting angles for the $+1$ charges are computationally arbitrary, any number of field lines from 11 to 13 can terminate on the negative charge, even though the correct value is 12. In Fig. 16, this boundary clumping effect makes the magnitude of the lower negative charge appear to exceed that of the upper charge by a ratio of 13:11.

A fuller explication of boundary clumping, including an algorithm that eliminates the effect from two-dimensional field line diagrams, will be presented in a subsequent work. For the moment we observe that boundary clumping may arise in charge distributions containing at least three point charges. Boundary clumping will therefore not be present in the field line diagrams associated with simple monopole or dipole distributions. The quadrupole, due to its high degree of symmetry, also lacks this effect. Boundary clumping should also be absent from charge distributions that include one positive charge and any number of negative charges, since a boundary, by definition, requires two distinct sources of field lines.[12]

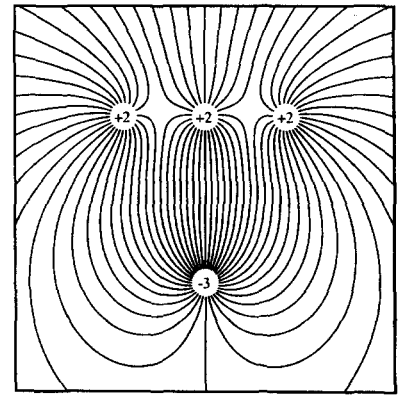

Fig. 15. Field line diagram for the distribution of Fig. 14, with the starting angles, θ_0, altered on the outermost positive charges to prevent boundary clumping.

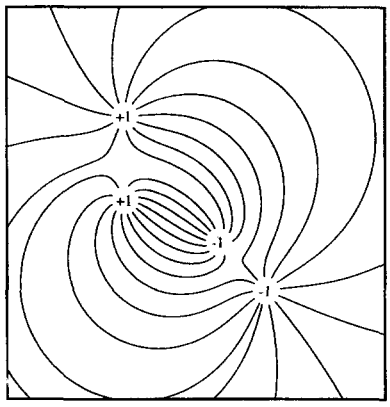

Fig. 16. Field line diagram with $1/r$ field, with boundary clumping resulting in an incorrect (unequal) number of field lines terminating on the two negative charges. Each $+1$ charge emits 12 field lines; the upper and lower -1 charges absorb, respectively, 11 and 13 field lines.

VIII. THREE-DIMENSIONAL FIELD LINE DIAGRAMS

As previously noted, one approach to avoiding projection effects is to represent three-dimensional $(1/r^2)$ electric fields by three-dimensional field line diagrams. While our computational scheme is easily extended to three dimensions, there are no perfectly satisfactory schemes for viewing the resulting field line diagrams. Both quasi-three-dimensional images, such as stereograms or holograms, and conventional two-dimensional projections of the three-dimensional field (which contain overlapping field lines) are likely to be visually ambiguous or overwhelming.

While it may be possible to resolve these practical issues, a more fundamental problem with three-dimensional diagrams relates to the creation of a uniform emission pattern on the spherical surface of a positive charge. In two dimensions, a uniform emission pattern containing any number of field lines is easily established by selecting an angular spacing that fits evenly into 2π radians. On the surface of a sphere, however, complete uniformity may only be achieved in a few cases, and for particular numbers of field lines. As with CFLDs, the result of incorrect field line spacing is that visual inspection of the field line diagram will fail to reveal the correct local field strength.

The problem of creating a uniform emission pattern is identical to the problem of uniformly "tiling" the surface of a sphere,[13] since one radial field line may be initiated at the center of each tiling element. For example, a uniform emission pattern containing 12 field lines is obtained by inscribing the sphere of the charge inside a dodecahedron, which contains 12 identical pentagonal faces. Uniformity in this context means, in part, that if any pentagon (field line) is rotated into the position of any other pentagon (field line), the tiling (global pattern of field lines) remains unchanged. This requirement, while necessary for uniformity, is clearly not sufficient. Consider, for example, a number of field lines equally spaced around the equator of a sphere. While the global field line pattern is invariant under the appropriate rotations around the polar axis, these equatorial field lines are clearly not uniformly distributed over the entire surface of the sphere. True surface uniformity requires that we also take the dispersion between adjacent field lines into account. The general formulation of this problem, which is beyond the scope of this work, is discussed in detail in Ref. 13. For present purposes we observe that uniformity, in the strictest sense, is only obtained by five tilings. These tilings employ the five regular polyhedra, otherwise known as the Platonic solids: the tetrahedron (four faces or field lines), the cube (6), the octahedron (8), the dodecahedron (12) and the icosahedron (20).

It is therefore impossible to create a completely uniform emission pattern on a sphere with other than 4, 6, 8, 12, or 20 field lines. If a "non-Platonic" emission pattern is selected, then, lacking uniformity of the emission pattern, there can be no expectation of uniformity of the termination pattern on negative charges. For some distributions Platonic emission patterns are simply unavailable. For example, if $N=4$, a tetrahedral tiling generates the emission pattern for a $+1$ charge. If the charge distribution also contains a $+4$ charge, however, there is no 16-faced Platonic solid available to generate its uniform emission pattern.

Even when Platonic emission patterns are available for each positive charge, Platonic termination patterns will often be impossible. For example, if an icosahedral emission pattern is used for each $+1$ charge in a charge distribution containing three $+1$ charges and a single -3 charge, the -3 charge cannot absorb these 60 lines uniformly, because there is no Platonic solid containing 60 faces. The solution in this particular case is to represent each $+1$ charge by a tetrahedral emission pattern, so the -3 charge can absorb the 12 field lines in a dodecahedral fashion. Even here, improper orientations of the emission patterns for the $+1$ charges would lead to boundary clumping on the -3 charge.

An apparent solution to the problem of obtaining uniform emission patterns from charges of different magnitudes is to construct charge distributions, as nature does, solely from charges of unity magnitude. A single choice of emission pattern, say icosahedral, can then be used for each elementary charge in the distribution. Unfortunately, while this eliminates nonuniformity at the spherical surface of the positive charges, the nonuniformity simply reappears in the adjacent region of empty space, reminiscent of the similar result for equatorial clumping illustrated in Fig. 9.

It would thus seem that there is a small but non-negligible set of charge distributions which can be properly represented with three-dimensional diagrams that use the five Platonic solids to represent the point charges. This assumes, however, that a uniform, Platonic emission pattern on positive charges results in a uniform, Platonic termination pattern on negative charges. Unfortunately, this is not the case except in a handful of special cases such as the dipole and linear quadrupole (and then only for a certain orientation of the emission patterns). The mapping of a region of solid angle (such as a "face" of a Platonic solid) from one charge to another, while area-preserving (up to a factor of $|q_+/q_-|$), is not shape-preserving; thus, the centers of Platonic solids on positive charges do not necessarily map to centers of faces of Platonic solids on negative charges. Gauss' law guarantees that a large number of field lines emitted uniformly from positive charges will land uniformly on negative charges; it does not guarantee that individual field lines originating from one particular point in space will terminate at another specified location. Figure 17, a stereogram of a three-dimensional field line diagram for a simple quadrupole, shows a rare case where Platonic emission and termination patterns can be produced. Each $+1$ charge emits six field lines uniformly from a cube, and the -2 charge absorbs all 12 lines uniformly on a

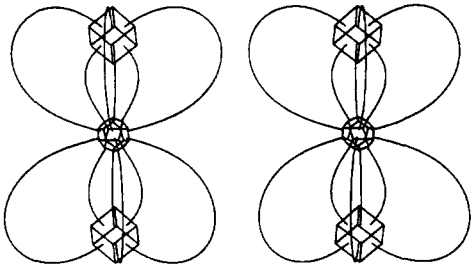

Fig. 17. Stereogram of a three-dimensional field line diagram for a linear quadrupole. Each field line begins in the center of one face of a cube, and terminates in the center of one face of the dodecahedron, confirming the perfect uniformity of the emission and termination patterns. The three-dimensional effect is achieved by relaxing one's eyes until the two images produce a combined central image, and then focusing on that image. Alternately, a central image is obtained by "crossing" one's eyes. The stereogram is best viewed from a distance of 6 to 10 in.

dodecahedron. We have not attempted to enumerate the class of charge distributions for which uniform emission and termination patterns on Platonic solids are possible, but we believe the class is small, containing at most a few distributions.

A different approach to solving the tiling problem is to relax our requirement of strict uniformity for the emission pattern. The spherical surface of each positive charge can then be covered with an almost arbitrary number of field lines that correspond to regions of equal solid angle, if not identical shape.[14] For example, field lines can be uniformly spaced in ϕ and $\cos(\Theta)$. The region of solid angle associated with each field line will vary in shape with Θ, however this effect can be reduced by increasing N, which increases the global density of field lines.

Boundary clumping may also be present in three-dimensional field line diagrams. As in the two-dimensional case, if field lines terminate on a negative charge from more than one source, the spacing of field lines at the resulting boundaries may incorrectly reflect the local electric field strength. In three dimensions, however, the field lines terminating on a negative charge from a specified positive charge define a region of surface area (a "patch") on the charge's spherical surface. An imprecise fit between adjacent patches may result in atypical spacing between a large number of field lines, and not just isolated pairs of lines. Since uniform termination patterns are rarely possible, boundary clumping can rarely be eliminated from three-dimensional diagrams. Figure 17 shows such a rare case, in which boundary clumping was avoided, and a perfect Platonic termination pattern achieved, by carefully selecting the three-dimensional orientation of the Platonic emission patterns.

IX. CONCLUSION

Electric field lines, while unphysical, have been thought to serve a useful role in field visualization.[15] There is a certain appeal to "reading" local electric field strength from a CFLD by visually estimating the local field line density. Unfortunately, CFLDs suffer from the projection effects of equatorial clumping and false monopole moment, as well as boundary clumping. Since these effects preclude the accurate visual estimation of field strength, CFLDs are of little utility for three-dimensional fields.

The failure of conventional field line diagrams has motivated us to explore the use of unconventional field line diagrams, such as diagrams representing two-dimensional fields and fully three-dimensional diagrams. While projection effects may be avoided, other problems remain, such as boundary clumping and the production of uniform three-dimensional tilings. It should be noted that each of the problems that we have considered is avoided by simply using graphical methods that do not employ continuous lines of force. For example, both the local direction and the local magnitude of a two-dimensional slice of an electric field can be accurately, although less aesthetically, represented by placing individual field vectors at the vertices of a square grid.

ACKNOWLEDGMENTS

Alan Wolf thanks Edward Spiegel and Tony Robbin for valuable discussions. Stephen J. Van Hook acknowledges the support of the NASA Graduate Student Researchers Program. Eric R. Weeks acknowledges the support of Office of Naval Research Grant No. N00014-89-J-1495 and an ONR Augmentation Award for Science and Engineering Training.

[a]E-mail:wolf@interport.net. Authors are listed alphabetically by institution.
[b]E-mail: svanhook@chaos.ph.utexas.edu
[c]E-mail: weeks@chaos.ph.utexas.edu

[1]"No observable electromagnetic phenomenon can exist which involves two points in space, and which depends upon there being a *continuous* line of force joining the points. Such a phenomenon could contradict our postulate of the complete sufficiency of the local vector fields for describing local phenomena." Joseph Slepian, "Lines of Force in Electric and Magnetic Fields," Am. J. Phys. **19**, 88 (1951).

[2]Some texts demonstrate that field strength is quadratically related to field line density in the CFLD of an isolated point charge. Since these discussions are limited to the monopole, the reader may be left with the impression that the quadratic relationship, or some consistent relationship, holds in the case of more complex charge distributions.

[3]Besides the inherent problems of CFLDs, such as limited spatial resolution, many of the CFLDs found in elementary texts are incorrectly drawn. See Leo Kristjansson, "On the drawing of lines of force and equipotentials," Phys. Teacher **23**, 202–206 (1985).

[4]The field lines for a dipole are determined analytically in Ref. 3, pp. 205–206.

[5]Electric Field Plotter (Physics Academic Software), which employs an algorithm similar to the one described in Sec. III, produces CFLDs that exhibit equatorial clumping. More commonly, electric field plotters, such as EM Field (Physics Academic Software), only draw field lines through user-specified points in space, and therefore do not attempt to convey field strength through two-dimensional field line density.

[6]There has been some confusion regarding the relationship between the magnitude of a point charge and the number of field lines it emits or absorbs in a two-dimensional field line diagram. Dennis E. Kelly, "Computing E-field Lines," Phys. Teacher **18**, 463 (1980); Mario Iona, "Number of Lines of Force," Phys. Teacher **19**, 354 (1981); Dennis E. Kelly, "A Common Misconception," Phys. Teacher **19**, 463 (1981). The relationship must be a linear one. Consider two $+1$ charges, each emitting N field lines. When observed at a distance much larger than the separation between the charges, the total electric field must resemble that of a single $+2$ charge. Since $2N$ field lines are seen to originate from a charge of apparently doubled magnitude, the relationship between charge and number of field lines must be linear. This result holds in both two and three dimensions. The contrary result of Kelly and Iona, which would have the $+2$ charge emit $\sqrt{2}N$ field lines, results from an incorrect comparison of uniform field line spacing in solid angle (in three dimensions) to uniform angular spacing within the plane.

[7]θ is the polar angle in the plane of the CFLD measured counterclockwise down from the y axis. ϕ is the azimuthal angle in the xz plane. This coordinate system is most convenient for discussing collinear charge distributions along the y axis.

[8]The sign-reversed $(-2, +4, -2)$ quadrupole provides further evidence that equatorial clumping misrepresents local field strength. Sign reversal,

whose only impact on the electric field is a global reversal of its direction, should not alter the relative spacing of field lines in a CFLD. Since the sign-reversed version of Fig. 6 must show uniform spacing of the outgoing field lines on the +4 charge, equatorial clumping does not show the invariance under charge reversal that would be expected of a true field property.

[9]Phillip M. Rinard, Delbert Brandley, and Keith Pennebaker, "Plotting Field Intensity and Equipotential Lines," Am. J. Phys. **42**, 792–793 (1974).

[10]While charge distributions lacking a monopole moment possess divergent field lines, such as the $\theta=0$ and $\theta=\pi$ lines in the dipole, such lines are few in number and can be avoided by the proper choice of θ_0. By contrast, the number of divergent lines associated with a false monopole moment is proportional to N, and is unaffected by the choice of θ_0. In several figures, including the dipole CFLD of Fig. 1(a), gaps on negative charges were avoided by setting θ_0 to a value very close to 0, producing an apparently divergent field line that eventually reappears at the opposite end of the diagram and terminates on a negative charge.

[11]Edwin A. Abbot, *Flatland: A Romance of Many Dimensions by a Square* (Seeley & Co., London, 1884). For a more technical discussion of two-dimensional science, see A. K. Dewdney, *The Planiverse: Computer Contact with a Two-dimensional World* (Poseidon, New York, 1984). While this article was in press, the authors were made aware of the recent note of T. E. Freeman, "One-, two-, or three-dimensional fields?," Am. J. Phys. **63**, 273–274 (1995). Freeman shows a field line diagram with a false monopole moment and correctly observes that the distortion would disappear in a two-dimensional universe.

[12]Boundary clumping can be avoided in a distribution with one negative and several positive charges by reversing the sign of each charge. A form of boundary clumping can be seen in charge distributions containing a single positive charge, but the problem originates solely from numerical errors that are easily avoided.

[13]The problem of distributing points uniformly on a sphere is discussed in the Internet document sphere.faq, produced by Dave Rusin. The document is located at: http://www.math.niu.edu:80/~rusin/papers/spheres/sphere.faq. Uniform tilings are not achieved on golf balls or geodesic domes which either employ multiple tiling elements or contain defects at the north pole or at the equatorial "weld" line.

[14]Reference 13 describes methods of obtaining nearly uniform distributions of an arbitrary number of points on the surface of a sphere.

[15]If field line diagrams are seen as primarily serving visualization and pedagogic purposes (rather than serving as a practical research/design tool) it may be time to reevaluate their pedagogic worth. Tornkvist *et al.* suggest that, independent of any imperfections that may be present in CFLDS, students often misinterpret these diagrams. S. Tornkvist, A. Petterson, and G. Transtromer, "Confusion by representation: On students' comprehension of the electric field concept," Am. J. Phys. **61**, 335–338 (1993).

Resonant Faraday rotation as a probe of atomic dispersion

D. A. Van Baak
Department of Physics, Calvin College, Grand Rapids, Michigan 49546

(Received 18 August 1995; accepted 4 December 1995)

The Faraday effect (the rotation of the plane of polarization of light as it propagates through a sample parallel to a static magnetic field) is readily detected in room-temperature rubidium vapor by a diode-laser experiment near the D_2 resonance line at 780 nm, and the theoretical treatment of this effect provides an unusually clear insight into the relation between absorption and dispersion in the interaction of light with matter. © *1996 American Association of Physics Teachers.*

I. INTRODUCTION

Impelled by a belief in the unity of the forces of nature, Michael Faraday sought, and in 1845 provided, the first phenomenological evidence for a connection between light and magnetism when he discovered the effect that still bears his name. He found that plane-polarized light, propagating through matter parallel to a static magnetic field, underwent a systematic rotation of its plane of polarization. The effect, though unambiguous, is typically not large, with rotation per unit distance per unit field of order 10 rad/m T ($\approx$0.03 arcmin/cm Oe) in ordinary glass samples in the midvisible; this "Verdet constant" is itself a function of wavelength, typically growing dramatically toward the blue end of the visible spectrum. Not until the atomic-electron hypothesis toward the end of the 19th century was it possible to provide a more detailed model for Faraday rotation; Becquerel predicted a Verdet constant related to the dispersion $dn/d\lambda$ of the material. A modern picture of Faraday rotation emerges from the quantum-mechanical response of an atom to a magnetic field; in this picture the atomic absorption and dispersion are both affected by the field, and in this sense the Faraday effect is to dispersion what the Zeeman effect is to absorption (or emission).

Given the small magnitude of Faraday rotation in bulk condensed matter, it might seem impossible to detect the effect for a much more dilute gas sample. It is the connection between absorption and dispersion that contradicts this expectation; both effects are subject to enormous enhancements near atomic resonances. This paper will work out the theory of Faraday rotation for light interacting with a simple model system, and will derive the behavior of the Verdet constant both far from, and very near, an atomic resonance. The calculation, in turn, is motivated by the possibility of observing resonant Faraday rotation in an atomic vapor, in this case by the interaction of 780 nm diode-laser radiation with a room-temperature sample of rubidium vapor. The notable and detailed agreement between observed rotation signals, and those computed from a theory involving atomic dispersion, demonstrates the reality of dispersion, and its intimate connection with absorption. Since the absorption and fluorescence of rubidium vapor under diode-laser excitation is an

